Design and Evaluation of a Novel 5 DoF Underactuated Thumb-Exoskeleton

Massimiliano Gabardi, Massimiliano Solazzi, Daniele Leonardis, and Antonio Frisoli

***Abstract*—This paper presents the design of a new exoskeleton for thumb. The main feature of this device is a high degree of underactuation. In fact, the 5 degrees of freedom (dof) of the thumb are actuated by just one linear actuator. Other features of the thumb-exos are its capability of exert only forces normal to the phalanx axis in the contact point, and its adaptability to different finger sizes. In this paper the spatial kinematic model is described and the link lengths are determined by means of a genetic algorithm (GA) over four basic grasping poses and the open hand pose. Finally, the thumb-exos mechanism was implemented and integrated in a full hand exoskeleton device. Performance of the thumb exoskeleton in terms of adaptation to different objects and hand sizes, and in terms of grasping forces have been evaluated through experiments and measuring muscular activity, grasping pressure and forces at different locations of the mechanism.**

***Index Terms*—Kinematics, Mechanism Design, Rehabilitation Robotics, Underactuated Robots, Wearable Robots**

I. Introduction

THE human hand is the most versatile gripper created by the nature. It is able to firmly grasp objects with different and complex shape thanks to the kinematics of its five fingers, powerful muscles, and a complex biological motor control system. From the kinematic point of view, the hand is composed by a ground part (the palm), four fingers with 4 dofs each, and a thumb. The thumb is the unique finger in the human hand with 5 dofs. Therefore, it is able to perform spatial movements such as its opposition to the other fingers of the hand, which is the basic movement of the grasping action. Because of its incredible complexity, in the last decades, the hand and in particular the human thumb have been widely studied from the kinematic point of view, and many kinematic models able to perform natural motions have been developed. In 1995 Giurintano et al. [1] proposed one of the first 5 link thumb model which entails non orthogonal and non incident axis for the carpo-metacarpal joint (CMC) and metacarpo-phalangeal (MCP) joint. Previous 3 link models use universal joints to model the CMC and MCP joints, leading to a non anatomically correct motion. The comparison between the error produced in the position of the trapeziometacarpal joint by using a 3 link model and a 5 link model has been investigated by Cerveri et al. in [2]. Other studies have been conducted in order to measure muscles arms at the thumb joints [3], or to define some kinematic properties, such as the kinematic parameters of the thumb carpo-metacarpal joint in [4]. An interesting study about the kinematic parameter of the thumb has been performed by Santos et al. in [5]. They investigate the anatomical variability in the Denavit-Hartenberg (D-H) parameaters of the human thumb. As results they clustered 3550 D-H parameters sets in four types of five links thumb models. Moreover, the distribution and the representative value for every D-H parameter for each type are provided. Since hand exoskeletons are developed in order to work combining their kinematics with the kinematics of the hand, the study of the human hand kinematics, especially of the thumb, is of particular interest for the development of effective devices. An example of hand-exos design based on both a hand model and a thumb motion analysis is presented in [6]. Hand exoskeletons can find their application in many different fields, ranging from the rehabilitation to the virtual reality interaction, therefore, in recent years, many hand-exoskeletons have been developed. Some devices have been designed in order to allow full posture control of the finger, therefore, they are able to control all the finger joints independently and provide full mobility during the grasping tasks [7], [8]; however, they mostly suffer from the heavy, bulky and high-cost design, sacrificing the wearability. In alternative one single actuator can be used to control the finger position as proposed in [9], or to control the pose of the fingers constraining the movement of one phalanx to the others, as shown in [10], [11]. Concerning the design of thumb exoskeletons, in literature it is possible to find different solutions proposed for the control of the 5 dofs human thumb. A 2 dofs device for controlling the CMC and MCP joints has been described in [12], whereas in [13], a full 5 dofs device able to control independently all the thumb joints is presented. Finally, in [14] a 4 dof cable driven underactuated thumb-exos device is proposed. In [14] two different actuators are used to independently drive the flexion-extension thumb motion and the adduction-abduction (AA) motion of the CMC joint of the thumb, whereas the AA motion of the MCP joint has been locked. Both the movements are guided by an underactuated cable driven kinematics. Recently, authors have developed an underactuated hand exoskeleton for all the fingers but the thumb [15], characterized by one actuator per finger, full mobility of the fingers, automatic hand size adaptability, possibility of grasping objects with different shape and size, efficient transmission of forces between the device and the fingers. In this work a novel thumb exoskeleton with the same characteristics but adjusted to the higher complexity of the thumb kinematics is presented (Figure 1). Moreover, data re-

Manuscript received: September, 10^{th}, 2017; Revised December, 20^{th}, 2017; Accepted January, 30^{th}, 2018.

This paper was recommended for publication by Editor Yasuyoshi Yokokohji upon evaluation of the Associate Editor and Reviewers' comments. This research was funded by project "CENTAURO" of the European Union Horizon 2020 Programme, Grant Agreement n. 644839.

Massimiliano Gabardi, Massimiliano Solazzi, Daniele Leonardis, and Antonio Frisoli are with Scuola Superiore SantAnna, TeCIP Institute, PERCRO Laboratory m.gabardi@sssup.it

Digital Object Identifier (DOI): see top of this page.

ported in [5] has been used within the design process to create a human thumb model integrated with the designed hand-exos device. The presented device is able to combine the advantages given by a powerful single motor actuation placed on the back of the hand, with a 5 dof kinematics able to guarantee the full mobility of the users thumb while wearing the device. The single actuation solution allows to reduce the weight and the volume occupied by the actuation system, whereas in order to guarantee the kinematic specifications the proposed device is based on a parallel kinematics featured by a high degree of underactuation. Furthermore such a parallel kinematics is designed to be able to adapt to different hand sizes. To the best of the authors knowledge, thumb-exoskeletons with such a high degree of underactuation has not been presented in previous works. In the following sections the requirements for the design of the thumb-exoskeleton are listed and the adopted design solutions are described. Successively, the solutions of both the inverse kinematics and the statics are described for the mechanical system composed by the thumb exos attached to the thumb finger. Those solutions have been implemented in a Genetic Algorithm (GA) in order to define the optimized link lengths for the kinematics. Finally, the experimental validation results obtained by testing the realized device on eight subjects with different hand size are presented.

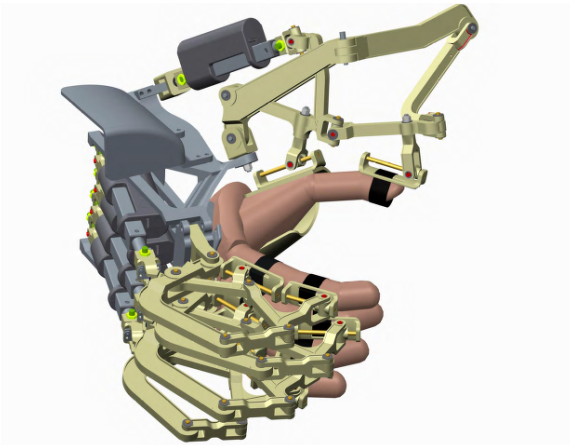

Fig. 1: CAD model of the integrated Thumb-exos device with the existing hand exos presented in [15].

II. The Thumb Exoskeleton

A. Design Requirements

As mentioned in the introduction the human thumb can be assumed as a serial kinematic chain able to perform complex spatial movements. Accordingly to the most recent literature the results provided in [5] are used to develop a 5 dofs kinematic model of the human thumb as a 5-link serial chain. The thumb model is used for testing the thumb-exos kinematics during the design process and guide the obtained result to the fulfillment of the following requirements: 1) Not to constrain any of the 5 dofs of the thumb when the user is wearing the exoskeleton device. 2) To guide the opening and the closure of the thumb allowing a natural motion of the finger. 3) To provide the user with an effective transmission of the forces to the thumb phalanges. 4) To ensure the self adaptability of the device to thumbs of different sizes. 5) To guarantee the possibility of integration with a hand-exos device grounded on the user's back of the hand.

B. Kinematics Features

The requirements for the new device define the guidelines followed for the design of the thumb kinematics. For the new thumb exoskeleton device a parallel spatial kinematics able to fulfill the mobility requirement is adopted, indeed the mechanical system composed by the human thumb wearing the exoskeleton has five non redundant dofs. Since the human thumb is part of the parallel kinematics loop the self-adaptability to a wide range of different thumb sizes is guaranteed and the discomfort caused in many devices by the misalignment between the thumb joints and the thumb-exos joints is avoided. Moreover, in order to design a kinematics able to guide both the opening and the closure of the thumb while adapting to the natural motions of the thumb itself, a kinematics with a high degree of underactuation is chosen for the new device. The thumb-exos is actuated by just one actuator. By means of the underactuated kinematics, in general, the only actuator of the thumb-exos applies torques to all the joints of the thumb, and at the same time the system maintains four dofs mobility (four different combined motions of all the thumb joints) when the actuator is locked. These four degrees of freedom allow the kinematics to adapt to different grasping poses of the thumb while the actuation supports the opening and closing forces. The provided mobility includes the capability of adapting to different natural motions (i.e. opening/closing on different planes) and objects of different size and shapes. Concerning the linear actuator, it has been inserted between an universal joint and a spherical joint in the kinematics in order to avoid the possibility of damage by a torque in any direction on the shaft. The effectiveness of the force transmission between the exoskeleton and the thumb depends by the design of the connection interfaces. The elasticity, softness and mobility of the skin make difficult to effectively provide the thumb with longitudinal forces and torques by means of fasteners. Therefore the device is designed in order to apply only normal forces to the phalanges. In particular, the presented thumb-exos exerts two forces on the thumb, one force is applied on the 1^{st} Metacarpal phalanx whereas the second force is applied on the Distal phalanx. Referring to figure 1, the joints which connect the kinematics and the thumb phalanges are equivalent to a spherical joint superimposed to a prismatic joint oriented like the phalanx direction. In this way just a force normal to the phalanx's axis can be exerted on the finger by the thumb-exos. The loads are applied on the guides which are rigidly connected to the thumb phalanges by means of fasteners. Moreover, in both the connections, the prismatic joint parallel to the phalanx axis ensures that the device can be properly worn on thumbs with different sizes keeping the same level of comfort for all the users. Finally, in order to achieve the possibility of integration with a hand-exos device, the kinematic chain has been designed to be grounded on a link (ground-link) rigidly mounted on the back of the users hand.

axis transition	θ	d	a	α
Z_0 to CMC(FE)	0	6.8	-1	-103.37
CMC(FE) to CMC(AA)	-92.57	-1	15.1	-69.59
CMC(AA) to MCP(AA)	28.89	15.4	35.6	-29.92
MCP(AA) to MCP(FE)	1.94	-18.9	10.3	100.93
MCP(FE) to IP(FE)	82.95	125.9	1	-21.63

TABLE I: Denavit-Hartenberg parameters adopted to realize the thumb model. The values in table are part of the results of the study reported in [5].

C. Inverse Kinematics Solution

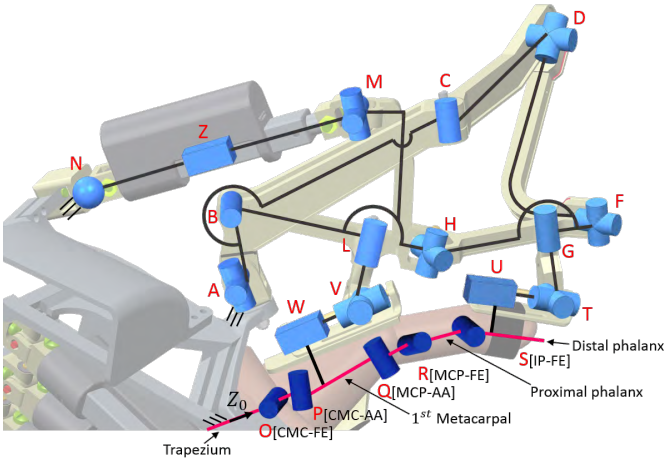

Fig. 2: Schematic representation of the Thumb-exos kinematics attached to the thumb kinematics. Prismatic joint Z is the only actuated joint of the kinematics.

The thumb-exos kinematics has been designed based on a realistic thumb model. The thumb kinematic model has been realized by following the Denavit-Hartenberg (D-H) parameters presented in [5] and reported in table I. Each group of four parameters (θ, d, a, α) allows to define the reference frame associated to each thumb joint by following the D-H convention. Referring to figure 2, the definition of the joint frames starts from Z_0, the ground reference attached to the trapezium, and it ends up to the Interphalangeal (IP) joint. In the table each joint has a tag depending on the kind of thumb motion it is responsible for, Adduction-abduction (AA) motion or Flexion-Extension (FE) motion. The D-H table defined in [5] has been used to develop a realistic CAD model of the thumb. Moreover the position of the thumb determined by the D-H table has been assumed as zero position for each joint. In the zero position the axes of the thumb phalanges are aligned. The phalanges lengths has been experimentally measured among 15 healthy subjects aged between 25 and 43. The mean value of 50.1 mm has been found for the 1^{st} Metacarpal whereas 36.6 mm has been obtained for the length of the Proximal phalanx and 25.2 mm for the Distal phalanx. The final scheme of the adopted kinematics for the realization of the thumb-exos is represented in figure 2. From the kinematic point of view the integrated system composed of the exoskeleton attached to the thumb is made up of six links (that belong to the exoskeleton) connected in parallel with the five links of the thumb model. Once defined the lengths of the links, the kinematic posture of the integrated system is completely defined by 5 joint coordinates (e.g.the pose of the thumb). The other 24 joint coordinates are determined by the solution of the inverse kinematics. Since the device is underactuated, it is possible to control just one of the 29 joint coordinates of the integrated system, it is the prismatic joint. With its motion the prismatic joint guides both the opening and closure of the thumb. In order to solve the inverse kinematics it is necessary to determine the spatial position and orientation of each joint of the mechanical system with respect to a ground coordinate system. A local reference frame has been associated to each joint according to the Denavit-Hartenberg convention and the homogeneous transformation matrix between each couple of successive joints has been determined. By composing the obtained homogeneous transformations four closed and independent loops through the joint frames have been determined. Referring to figure 2 the following independent loops have been defined:

$$ {}_BT^C\,{}_CT^D\,{}_DT^F\,{}_FT^H\,{}_HT^B = I \quad (1) $$

$$ {}_AT^B\,{}_BT^M\,{}_MT^Z\,{}_ZT^N\,{}_NT^A = I \quad (2) $$

$$ {}_AT^O\,{}_OT^P\,{}_PT^W\,{}_WT^V\,{}_VT^L\,{}_LT^B\,{}_BT^A = I \quad (3) $$

$$ {}_AT^O\,{}_OT^P\,{}_PT^Q\,{}_QT^R\,{}_RT^S\,{}_ST^U\,{}_UT^T\,{}_TT^G\,{}_GT^H\,{}_HT^B\,{}_BT^A = I \quad (4) $$

where the generic ${}_XT^Y$ represents the homogeneous transformation matrix from the joint reference associated to the joint X to the joint reference associated to the joint Y. The independency of the loops is guaranteed by their definition. Indeed, every loop includes at least two successive joints which are not included in any of the other loops. Finally, by imposing the coincidence condition between the first and the last frame of each loop it is possible to determine 24 equations in the 24 unknown joint coordinates. The solution of the inverse kinematics has been used to numerically test the device for different poses of the thumb and solve the static of the system for each evaluated pose.

D. Statics Solution

As stated before the thumb-exos exerts two forces on the thumb phalanges, one on the Metacarpal phalanx and one on the Distal phalanx. Because of the high level of underactuation it is not possible to independently control neither the intensity nor the direction of the forces. Equation (5) express the relation between the actuation force (F_a) exerted by the linear actuator (joint Z in fig. 2), which is the only actuated joint of the kinematics, and the 3-components spatial forces applied on the thumb phalanxes ($\vec{F}_1$ and $\vec{F}_2$).

$$ \begin{bmatrix} \vec{F}_1 \\ \vec{F}_2 \end{bmatrix} = \begin{bmatrix} J_1(\vec{q})_{3x1} \\ J_2(\vec{q})_{3x1} \end{bmatrix} F_a \quad (5) $$

$J_1(\vec{q})$ and $J_2(\vec{q})$ are 3x1 Jacobian matrices. The Jacobian matrices depend by $\vec{q}$. $\vec{q}$ is the vector of the positions assumed by all the 29 joints of the kinematics. Therefore both J_1 and J_2 can be evaluated once the inverse kinematics is solved. Because of the complexity of the kinematic problem both the inverse kinematics and the statics have been numerically evaluated. In section III the solution of the statics has been

used within the link lengths determination process in order to evaluate the fitness of an individual that belongs to the population of the genetic algorithm.

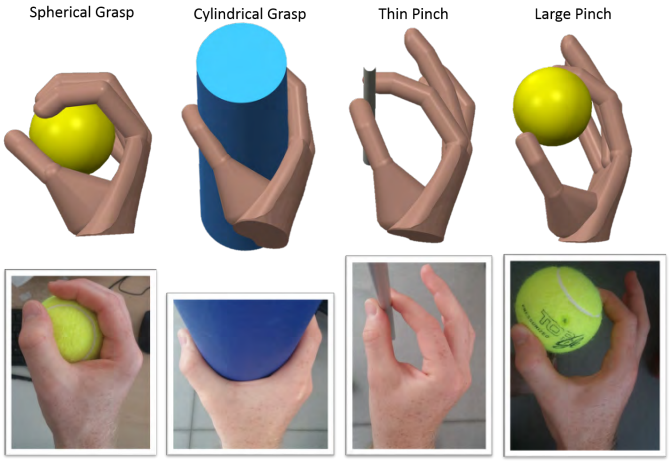

Fig. 3: CAD hand model and real hand grasping poses of different objects (a tennis ball (diameter 70 mm), a plastic cylinder (diameter 80 mm) and a metal cylinder (diameter 10 mm)).

III. Link Lengths Determination

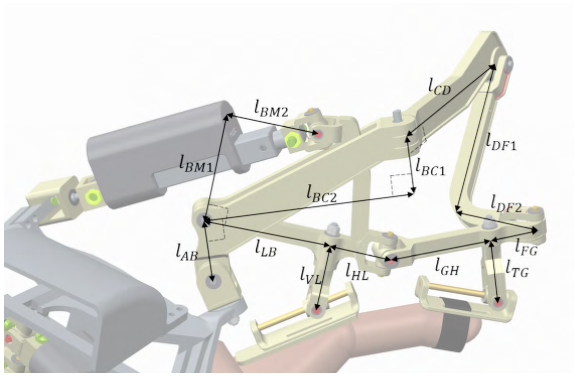

Fig. 4: Representation of the optimized lengths of the Thumb-exos device.

The aim of this section is to describe the way the lengths of the links have been determined in order to improve the performance of the resulting thumb-exos kinematics. The 14 lengths which determine the link shapes represented in figure 4 have been optimized by means of a genetic algorithm. The fitness function has been defined in order to obtain the following results:

- maximize the sum of the forces exerted on the thumb phalanges by the exoskeleton;
- minimize the difference between the two forces;

The starting values for the lengths have been determined by the first non optimized solution, that was experimentally obtained with a CAD software. These values are listed in the left column of table III. The optimization search space has been limited by assuming as lower limits 0.5*(starting lengths) and as upper limits 1.5*(starting lengths). This limits have been chosen in order to look for solutions in a reasonably wide search space limiting the lengths combinations that lead to a too much different kinematics or non mechanically feasible kinematics that numerically show better performances. The performance of the system has been evaluated on the open hand pose plus four common grasping poses. The coordinates of the thumb joints for each of the five poses have been determined by visually comparing the thumb CAD model defined in section II-C with the pictures of a hand performing the four grasping poses (figure 3). Referring to figure 3 the thumb kinematics has been optimized in the following grasping poses: *spherical grasp*, *large pinch*, *cylindrical grasp*, *thin pinch* and the *open hand* pose. With respect to the zero position the joint angles of the thumb joints are listed in table II for each grasping pose. As previously mentioned, the optimization has been performed by means of a genetic algorithm. The designed genetic algorithm works with a population of 100 individuals. Moreover, a stall generation limit is adopted as convergence criteria. In detail, the algorithm is programmed to stop when the cumulative change in the fitness function value over 10 generations is less than 0.0001. The adopted GA fitness function (FF) is shown in equation 6. It is defined as the mean of a performance parameter (PP) evaluated over the five testing poses.

Pose	CMC (FE)	CMC (AA)	MCP (AA)	MCP (FE)	IP (FE)
open hand	-10	10	-1.37	32.13	12.7
spherical grasp	34.46	-37.22	7.7	38.27	37.77
cylindrical grasp	20	-30	-5	5	45
large pinch	10	-28.32	1	15	30
thin pinch	35	-22	-5	10	30

TABLE II: Thumb joint angles for the five grasping poses with respect to the zero position expressed with the D-H table.

$$FF = \frac{\sum_{i=1}^{5} PP_i}{5} \tag{6}$$

$$PP_i = \frac{1}{|\vec{F}_i| + |\vec{f}_i|} + W_1 \frac{|\vec{F}_i|}{|\vec{f}_i|} + W_2 P_i \tag{7}$$

Equation (7) shows how the performance parameter (PP) is defined. Referring to equation (7), PP_i is the performance parameter evaluated for the i^{th} grasping pose, F_i and f_i are respectively the major and the minor force exerted on the thumb phalanges and evaluated by solving the statics of the system. W_1 and W_2 are two arbitrary weights assumed experimentally for this optimization as 10 and 5 respectively. Finally, P_i is a penalty value. The PP is the sum of three components. The first component is the inverse of the sum of the two forces exerted by the exoskeleton on the thumb, whereas the second component is proportional to their ratio and by definition is always grater than one. The last component is proportional to the penalty value. The penalty value P_i is non-zero when at least one of the three prismatic joint coordinates is out of its admissible range. Every time the inverse kinematics is solved for a population individual within the genetic algorithm and the PP_i is evaluated for each of the testing poses, the penalty value assigned to that individual is the sum of the absolute values of the possible overshoots of each of the three prismatic joints of the kinematics with respect

label	starting length [mm]	min. search space [mm]	max. search space [mm]	optim. length [mm]
l_{AB}	35	17.5	52.5	30.24
l_{BM1}	49.4	24.7	74.1	52.87
l_{BM2}	32.7	16.35	49.05	42.44
l_{BC2}	72.5	36.25	108.75	95.33
l_{BC1}	45.5	22.75	68.25	25.79
l_{CD}	140	70	210	102.46
l_{DF2}	77	38.5	115.5	40.98
l_{DF1}	57	28.5	85.5	82.51
l_{FG}	29.8	14.9	44.7	22.12
l_{GH}	55.1	27.55	82.65	51.13
l_{HL}	35	17.5	52.5	26.31
l_{LB}	60	30	90	59.77
l_{VL}	21.5	10.75	32.25	31.45
l_{TE}	34.5	17.25	51.75	31.59

TABLE III: Starting lenghts used to run the optimization GA process (left column), GA search space limits and optimized lengths obtained as output of the genetic algorithm (right column).

Pose	Starting Solution		Optimized Solution	
	$F1$	$F2$	F1	F2
open hand	0.83	0.28	0.47	0.48
spherical grasp	0.89	0.23	0.38	0.38
cylindrical grasp	1.64	0.26	0.54	0.35
large pinch	1.26	0.21	0.38	0.39
thin pinch	1.26	0.26	0.41	0.32

TABLE IV: Force values evaluated by adopting the starting lengths and adopting the optimized lengths. Forces are calculated for a unitary actuation force.

to their limits. The admissible ranges for the prismatic joint coordinates have been assumed as:

- 0-60 mm for the slider on the metacarpal phalanx
- 0-40 mm for the slider on the distal phalanx,
- 123-173 mm for the actuated prismatic joint.

The difference between the limits assumed for the actuated prismatic joint represents the maximal stroke of the adopted linear actuator, which is 50 mm.

In table III, the obtained optimized lengths are listed in the right column. The results of the optimization has been reported in the right column, whereas the starting guess in the left column. It is possible to notice that none of the optimized lengths is on the boundary of the search space. The fitness function obtained with the optimized lengths significantly improved. Indeed, $FF_{start} = 50.6363$ is the fitness function value obtained by the thumb exos kinematics evaluated with the starting link lengths, whereas after the optimization the value $FF_{optim} = 24.07$ is obtained. Concerning the effect of the optimization on both the forces exerted by the exoskeleton on the two phalanges. In table IV, the force values obtained for a unitary actuation force are listed for each evaluated pose. The values are reported for both the kinematics defined by the starting link lengths and the optimized kinematics. It is possible to notice that in the optimized solution the obtained force values are similar among the five grasping poses, moreover, for each pose, F1 is similar to F2 as expected. Referring to the numerical results in table IV, in the 5 evaluated poses, the Thumb-exos device is able to provide for a unitary actuation force (1N) a force of at least 0.38 N on the 1st metacarpal (F1) and a force of at least 0.32 N on the distal phalanx (F2) of the user. At the maximum actuation force of the adopted actuators (50N), the two forces become F1max = 19N and F2max = 16N.

A. *Thumb-Exos Structural Design*

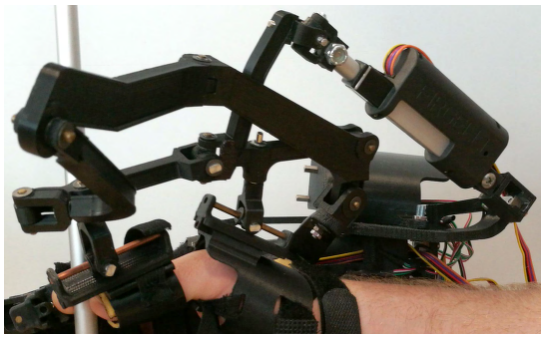

Fig. 5: The thumb-exos prototype.

Figure 5 shows the realized prototype of the thumb exoskeleton. In order to reduce the total weight of the device, the links are printed in light material by means of a rapid prototyping 3D printer. Moreover, in order to improve the comfort and the wearability, the entire ground link has been modeled over a 3D reconstruction of a real hand acquired with an RGB-D Kinect camera. In this way an ergonomic shape for the contact surface has been obtained leading to a more natural contact between the interface and the back of the users hand. A layer of foam on this surface will improve the adaptability of the ergonomic interface to different hand sizes and the adherence between the device and the back of the hand. All the joints but the spherical are realized by custom aluminum pins coupled with low friction plastic bushings in order to reduce the friction load on the thumb while it is moving. The spherical joint at the base of the actuator and the actuator itself are commercial component integrated in the kinematics design process. A Firgelli P16 linear actuator (DC motor with screw mechanism, 50N stall output force, 50 mm stroke) was chosen to actuate the thumb, and was coupled with a miniaturized strain-gauge 1 dof force sensor (SMD Sensors S215, 55 N full scale) mounted at the base of the actuator. Concerning the transmission of the forces to the thumb, because of the perpendicularity between the forces transmitted and the phalanx axes, the fasteners don't need to be excessively tight around the finger to effectively load the thumbs phalanges and not to move from the starting position. This kinematic feature allows to improve the level of comfort perceived by the user while he is wearing the device. Referring to figure 5 it is possible to notice that the fasteners are composed by a rigid 3D printed part kept in position by one or more fabric stripes. In particular, one stripe is used to keep the thimble attached to the distal phalanx, whereas two fabric stripes are used to keep the ergonomic plastic part attached to the 1^{st} metacarpal, one stripe is wrapped around the phalanx close to the joints and the other is wrapped around the wrist.

IV. Experimental Methods

Two different experimental sessions have been conducted in order to evaluate the developed mechanism for the thumb exoskeleton: the first aimed to qualitatively evaluate functionality of the exoskeleton in grasping objects of different shape and size. The second experiment involved different hand sizes and made used of position, force, pressure and EMG sensors in order to investigate propagation of forces during a grasping and releasing sequence of operation. In the first experiment eight healthy subjects (male, age between 25 and 31) wore the whole hand exoskeleton, composed of the finger mechanisms presented in [15] and of the here proposed mechanism for the thumb. Each subject was seated in front of a desk and the exoskeleton was held by a fixed support. Due to the non-backdrivability of the actuators, a simple force control was implemented to operate the device. The algorithm closed a control loop between the reference voltage supplied to each DC linear actuator and each strain gauge force sensor mounted between the actuator and the chassis of the exoskeleton. The control algorithm was executed at 250 Hz on a Beagleboard microcontroller board and Texas Instruments DRV8835 H-bridge ICs were used to drive the actuators. The control loop enabled the user to actively move the fingers and the exoskeleton in transparency and to test finger closure and the grasping stability on the same objects used for the optimization procedure.

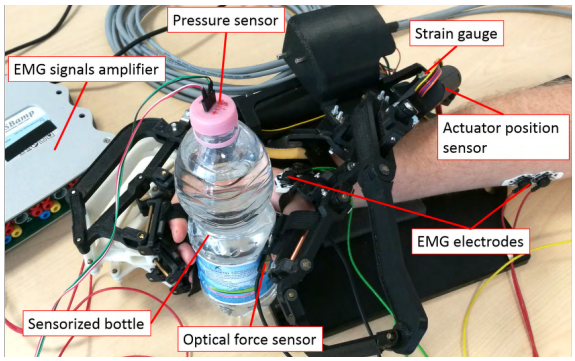

Fig. 6: The experimental setup.

The second experimental session investigated forces applied by the exoskeleton in grasping and releasing tasks with different hand sizes. In this experiment, a pressure sensorized water bottle (presented in [11]) was used to measure the overall pressure exerted by the hand during grasping. A miniaturized optical force sensor (OptoForce OMD-10-SE-10N, range 10N, resolution 1 mN) was implemented to measure contact forces between the thumb and the object. The strain gauge sensor at the base of the actuator and the linear potentiometer integrated inside the actuator provided also information about force and displacement applied at the actuator level. Additionally, EMG signals were acquired in bipolar configuration in proximity of the Adductor Pollicis muscle, in order to monitor muscle relaxation during the active exoskeleton operation. Similarly to the previous experiment, subjects wore the whole hand exoskeleton. They were seated in front of a desk and the exoskeleton was held by a support (Figure 6). A preliminary experimental phase was conducted with one healthy subject (male, age 28), and evaluated forces exerted by muscles during a natural and stable grasping of the sensorized object. In this phase the exoskeleton was controlled in transparency modality (similarly to the previous experiment) and the subject was asked to actively grasp and release the sensorized object ten times. He was asked to apply the amount of force he felt comfortable for a stable grasping. In the next experimental phase, the reference voltage fed to the actuator of the thumb was set to resemble the maximum contact force measured during the preliminary experimental phase. In the final experimental phase, the subject's hand was held completely passive and the actuator actively assisted the closing and opening of the thumb. Eight healthy subjects participated to the experiment (male, age between 25 and 31) with different hand sizes as reported in Table V. A feedforward reference voltage was fed to the actuator, shaped as shown in figure 9, in order to slowly close and open the thumb. The sequence was repeated ten times for each subject. Subjects were asked to keep the hand completely relaxed and the rectified and filtered EMG signal was monitored to be below 30 uV throughout the closing phase (according to results measured in the preliminary experimental phase).

Subject	Thumb [cm]	1^{st} Met. [cm]	Proximal [cm]	Distal [cm]
1	10.1	3.8	3.6	2.7
2	10.8	4.5	3.5	2.8
3	11	4.3	3.9	2.8
4	11.2	4.7	3.4	3.1
5	12.4	5.3	3.8	3.3
6	12.9	4.6	4.7	3.6
7	13	5.6	4	3.4
8	13.5	5.4	4.7	3.4

TABLE V: Subjects thumb sizes measured on the back hand side from the 1^{st} Metacarpal base to the top of the thumb while aligned to the forearm and dimensions of the thumb phalanges (1^{st} Metacarpal, Proximal and Distal).

V. Experimental Results and Discussions

Regarding the first experimental session, involving grasping of objects with different size and shape, all the eight subjects (Table V) achieved a stable grasping for all the tested objects. Figure 7 shows the grasping poses assumed by subject 2. Fingers and the thumb mechanism could adapt to the object surface and each object was held lifted off the surface of the table. Although the grasping was actively driven by the subjects and the exoskeleton did not provide any guidance or assistance to the grasping, it shows the proposed mechanism, thanks to its high mobility, could adapt to objects of different shape and size and to different thumb sizes. Regarding the preliminary phase of the second experiment, a feed-forward voltage profile, reported in Figure 9 was obtained for driving the actuator in order to resemble, in the robotic driven modality, the contact force measured during the muscle-driven grasping and opening sequence. It has to be noted that the reference provided to the actuator corresponded to the 20% of the maximum actuator output force. Since the actuator

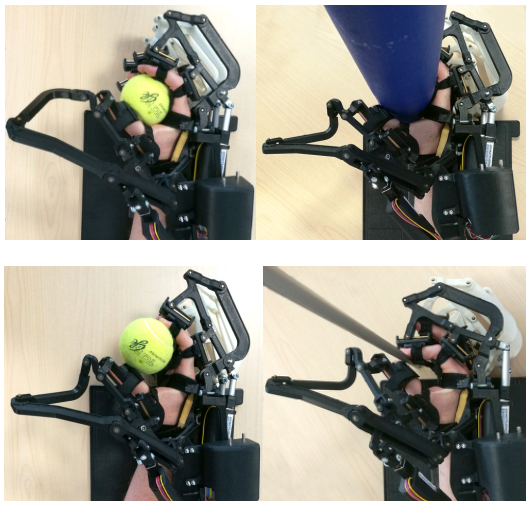

Fig. 7: Hand grasping tests

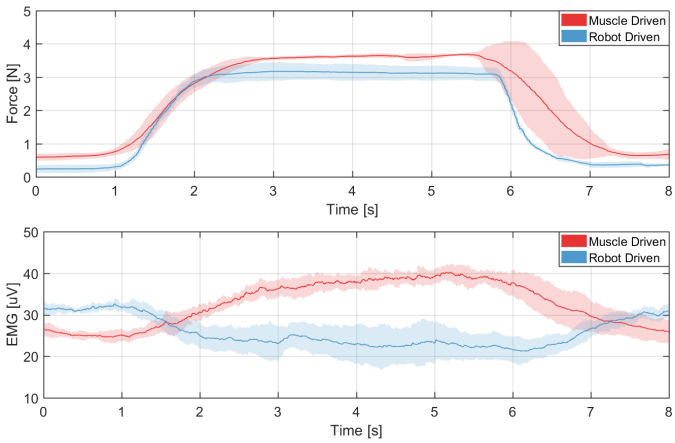

Fig. 8: (a) Measured thumb contact force and (b) rectified and filtered EMG signals of the Adductor Pollicis during the active (Muscle Driven) and passive (Robotic Driven) closing of the thumb, averaged over ten repetitions

was fed with the same feed-forward reference voltage profile, at stall the estimated output force of the actuator was the same for all repetitions. Graph in Figure 8a show comparable maximum contact forces, averaged over ten repetitions, for both the muscle driven and robotic driven modalities (maximum measured contact force: 3.68 N muscle driven, 3.11 N for the robotic driven). Regarding the recorded muscle activity, graph in Figure 8b show noticeable activation of the

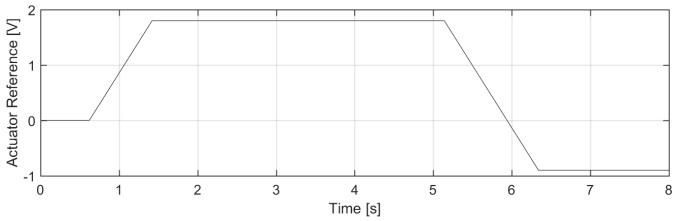

Fig. 9: Reference voltage fed to the thumb actuator in order to actuate the closing and opening sequence

Adductor Pollicis during the grasping phase of the muscle driven modality (40 uV) with respect to the relaxed hand of the robotic driven modality (25 uV). EMG signals were rectified and filtered (low-pass filter, 3 Hz cut-off frequency). Also, in the robotic driven modality EMG activity is at minimum during the grasping phase but conversely slightly increases during the opening phase (32 uV). This might be caused by residual resistance opposed by muscles during the full robotic-driven opening of the thumb. Regarding results of the second experimental phase, for all the eight subjects the thumb mechanism was able to assist a complete grasping and opening sequence with similar behaviour, as shown in graphs of Figure 10. In particular the graph related to position of the linear actuator in Figure 10a shows a transient period corresponding to the thumb going in contact and pressing the sensorized object. After the initial transient period the position of the linear actuator stabilizes for all the subjects. Different linear dimensions, corresponding both to different deformations of the grasped object and different configurations of the thumb mechanism. Estimated output force of the linear actuator was in line with measurement of the strain gauge force sensor mounted at the base of the actuator, as shown in Figure 10b. Regarding the measured contact force and the overall pressure exerted on the grasped object, output values varied also due to different thumb sizes, resulting in different configurations of the thumb mechanism and different propagation of forces. The profile of the contact force was comparable between subjects (Figure 10c), although with different amplitudes: the relative difference was of 38.2% (between Subject 6 and Subject 4) of the maximum contact force. Regarding the overall grasping pressure shown in Figure 10d, the relative difference was 33.2% (between Subject 3 and Subject 1) of the maximum measured pressure. No trends between the thumb length of different subjects and the measured contact force or grasping pressure were noted. This suggest that the length of the thumb phalanxes is a parameter that does not completely describe the hand shape and the consequent system behavior, although useful for the design of the exoskeleton kinematics. Other factors might affect the propagation of forces during grasping, such as different thumb thickness and different stiffness of tissues (tendons and muscles). Moreover human joints do not represent ideal revolute joints, and pose (joint angles) and kinematics can vary between subjects. Overall, the behaviour of the thumb-exos showed to be compliant with the set of different thumb sizes measured in the experiment, and no critical working conditions emerged with any of the enrolled subjects.

VI. Conclusions

In this paper the design and the optimization of a novel underactuated thumb exoskeleton with 5 degrees of freedom and one actuator are presented. Thanks to its kinematics and in particular to the four underactuated dofs, the device is able to guide the motion of the thumb allowing a natural movement. Furthermore, important points such as the adaptability to different hand sizes, the wearability and the comfort have been taken into account in the design process.

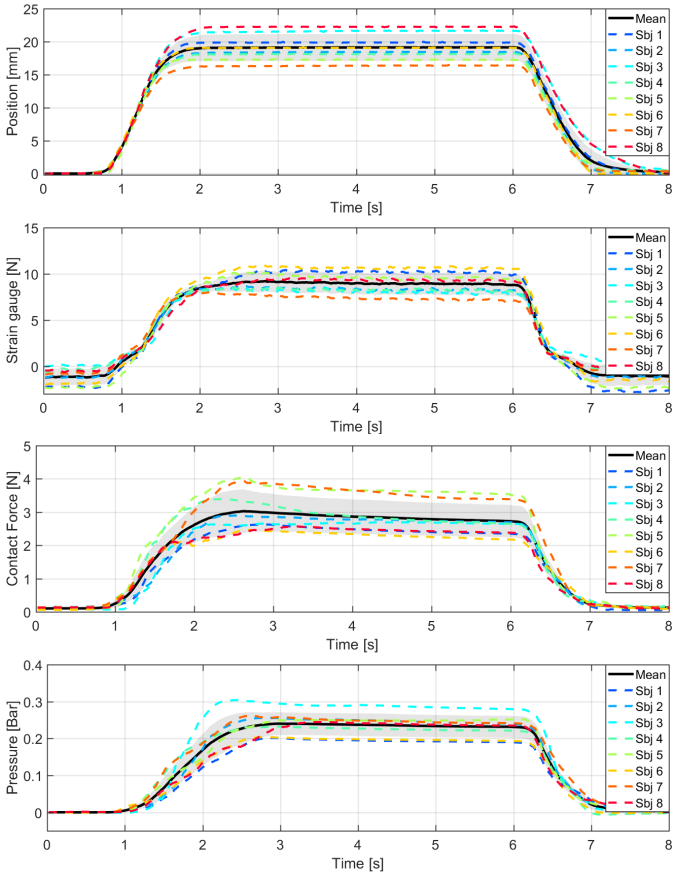

Fig. 10: (a) position of the linear actuator, (b) force at the actuator strain gauge sensor, (c) force at the contact point and (d) pressure of the grasped object measured during closing and opening sequence and averaged over ten repetitions.

Adaptability do different hand size was achieved adopting an open kinematic design that closes on the finger phalanges of the users. Moreover, the link lengths of the device have been optimized in order to assure the correct statics behavior in grasping tasks, especially in five poses representing typical grasping configurations. Although in this work the aim was to optimize the grasping performance of the device, it has to be noted that different optimization criteria might be used: reduction of the overall dimensions of the device could be a reasonable choice in order to improve the wearability and the portability. Also, further kinematic synthesis analysis could be performed in order to find whether some links combination of the thumb-exos, showing relevant overall dimensions, could be substituted by more compact mechanism with the same kinematic behavior. Finally, the results of experimental tests on the realized prototype are provided. Both the grasping motion capability of the device actively driven by the subject and the grasping forces exerted in the active condition (with passive user's hand) have been evaluated by measuring propagation of forces from the actuator to the grasped object and by monitoring muscle activity. The experiments showed adaptability of the device to different hand sizes, with a stable grasping achieved by all the subjects and with comparable output forces and grasping pressure.

ACKNOWLEDGMENT

This research was funded by project "CENTAURO" of the European Union Horizon 2020 Programme, Grant Agreement n. 644839.

REFERENCES

[1] D. Giurintano, A. Hollister, W. Buford, D. Thompson, and L. Myers, "A virtual five-link model of the thumb," *Medical engineering & physics*, vol. 17, no. 4, pp. 297–303, 1995.

[2] P. Cerveri, E. De Momi, M. Marchente, N. Lopomo, G. Baud-Bovy, R. Barros, and G. Ferrigno, "In vivo validation of a realistic kinematic model for the trapezio-metacarpal joint using an optoelectronic system," *Annals of biomedical engineering*, vol. 36, no. 7, 2008.

[3] W. P. Smutz, A. Kongsayreepong, R. E. Hughes, G. Niebur, W. P. Cooney, and K.-N. An, "Mechanical advantage of the thumb muscles," *Journal of biomechanics*, vol. 31, no. 6, pp. 565–570, 1998.

[4] L. Y. Chang and N. S. Pollard, "Method for determining kinematic parameters of the in vivo thumb carpometacarpal joint," *IEEE Transactions on Biomedical Engineering*, vol. 55, no. 7, 2008.

[5] V. J. Santos and F. J. Valero-Cuevas, "Reported anatomical variability naturally leads to multimodal distributions of denavit-hartenberg parameters for the human thumb," *IEEE Transactions on Biomedical Engineering*, vol. 53, no. 2, pp. 155–163, 2006.

[6] T. Burton, R. Vaidyanathan, S. Burgess, A. Turton, and C. Melhuish, "Development of a parametric kinematic model of the human hand and a novel robotic exoskeleton," in *Rehabilitation robotics (ICORR), 2011 IEEE international conference on*. IEEE, 2011, pp. 1–7.

[7] J. Li, R. Zheng, Y. Zhang, and J. Yao, "iHandRehab: An interactive hand exoskeleton for active and passive rehabilitation," in *IEEE International Conference on Rehabilitation Robotics (ICORR)*, 2011.

[8] Y. Hasegawa, J. Tokita, K. Kamibayashi, and Y. Sankai, "Evaluation of fingertip force accuracy in different support conditions of exoskeleton," in *IEEE International Conference on Robotics and Automation (ICRA)*, 2011, pp. 680–685.

[9] J. Iqbal, N. Tsagarakis, and D. Caldwell, "A multi-DoF robotic exoskeleton interface for hand motion assistance," in *IEEE International Conference of the Engineering in Medicine and Biology Society*, 2011.

[10] A. Chiri, N. Vitiello, F. Giovacchini, S. Roccella, F. Vecchi, and M. Carrozza, "Mechatronic design and characterization of the index finger module of a hand exoskeleton for post-stroke rehabilitation," *IEEE/ASME Transactions on Mechatronics*, vol. 17, no. 5, 2012.

[11] D. Leonardis, M. Barsotti, C. Loconsole, M. Solazzi, M. Troncossi, C. Mazzotti, V. P. Castelli, C. Procopio, G. Lamola, C. Chisari *et al.*, "An emg-controlled robotic hand exoskeleton for bilateral rehabilitation," *IEEE transactions on haptics*, vol. 8, no. 2, pp. 140–151, 2015.

[12] D. Guilherme N. DeSouza, P. Aubin, K. Petersen, H. Sallum, C. Walsh, A. Correia, and L. Stirling, "A pediatric robotic thumb exoskeleton for at-home rehabilitation: The isolated orthosis for thumb actuation (iota)," *International Journal of Intelligent Computing and Cybernetics*, vol. 7, no. 3, pp. 233–252, 2014.

[13] F. Wang, C. L. Jones, M. Shastri, K. Qian, D. G. Kamper, and N. Sarkar, "Design and evaluation of an actuated exoskeleton for examining motor control in stroke thumb," *Advanced Robotics*, vol. 30, no. 3, pp. 165–177, 2016.

[14] M. Cempini, M. Cortese, and N. Vitiello, "A powered finger–thumb wearable hand exoskeleton with self-aligning joint axes," *IEEE/ASME Transactions on Mechatronics*, vol. 20, no. 2, pp. 705–716, 2015.

[15] M. Sarac, M. Solazzi, E. Sotgiu, M. Bergamasco, and A. Frisoli, "Design and kinematic optimization of a novel underactuated robotic hand exoskeleton," *Meccanica*, vol. 52, no. 3, pp. 749–761, 2017.